CHAPTER 5
BIOLOGY

During the course of our studies on the rearrangement reaction, a series of 1*H*- and 2*H*-indazolylpyridinium derivatives were prepared. These indazolylpyridinium derivatives are precursors to the corresponding tetrahydropyridinyl species which are potential MAO substrates. At the completion of this work, the reduction of the pyridinium derivatives to the corresponding tetrahydropyridines remained to be carried out. Determination of MAO-A and MAO-B substrate properties of these compounds are expected to provide valuable information regarding the active sites of these enzymes. Also, the potential "prodrug" properties of substituted tetrahydropyridinylindazoles may provide an opportunity for *in vivo* neuroprotection studies.

Previously, MAO-B substrate properties of synthetically accessible "prodrugs" of nitroindazoles had been investigated.[217] We review the results of these studies briefly here. Also the MAO-A substrate properties of these compounds will be presented in relation to the possible factors leading to MAO-A or MAO-B selectivity. First, a brief review of the studies on the active site of both forms of MAO will be given.

5.1. MAO Active Site

The X-ray crystal structure of MAO-B was not available until very recently[218] and efforts to obtain a crystal structure for MAO-A have not been successful thus far. Therefore, active site models of the MAOs have been developed with the aid of structure activity relationship (SAR) studies using both inhibitors and substrates. Most of these attempts utilize MAO inhibitors rather than substrates. These modeling attempts will be summarized briefly.

---

[217] Reference 1, pages 108-110 and 120-128.
[218] Claudia, B., Newton-Vinson, P., Hubalek, F., Edmondson, D., Mattevi, A. (2002) Structure of human monoamine oxidase B, a drug target for the treatment of neurological disorders *Nat Struct. Biol.* **9**, 22-26.

5.1.1. Modeling of MAO Active Site Based on the Structure of Inhibitors

Thulle *et al.* proposed a model of the MAO-A active site using comparative molecular field analysis (CoMFA) based on the structural features of a series MAO-A selective inhibitors possessing isoquinoline (**239**), dihydroisoquinoline (**240**) or tetrahydroisoquinoline (**241**) as the pharmacophore.[219] In this model steric as well as polar properties of isoquonolines and other MAO-A inhibitors from the literature were utilized. They have concluded that electrostatic forces as well as steric, lipophilic and hydrophobic interactions are critical for MAO-A inhibition.

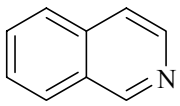

239

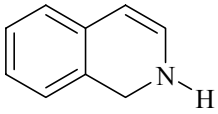

240

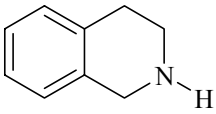

241

The structural features of reversible MAO-A inhibitors with antidepressant properties, toloxatone (**23**), moclobemide (**24**), brofaromine (**242**), harmine (**243**), and R40519 (**244**) and were investigated by Moureau *et al.*[220] In this study, special emphasis was given to the interaction of these planar MAO-A inhibitors with the flavin of the enzyme as a possible mechanism of inhibition.

---

[219] Thull, U., Kneubuehler, S., Gaillard, P., Carrupt, P.-A., Testa, B., Altomare, C., Carotti, A., Jener, P., McNaught, K.St.P. (1995) Inhibition of monoamine oxidase by isoquinoline derivatives: qualitative and 3D-quantitative structure-activity relationshops *Biochemical Pharmacology* **50**, 869-877.

[220] Moureau, F., Wouters, J., Depas, M., Vercauteren, D.P., Durant, F., Ducrey, F., Koenig, J.J., Jarreau, F.X. (1995) A reversible monoamine oxidase inhibitor, tolaxatone: comparison of its physicochemical properties with those of other inhibitors including brofaromine, harmine, R40519 and moclobemide. *European Journal of Medicinal Chemistry* **30**, 823-838.

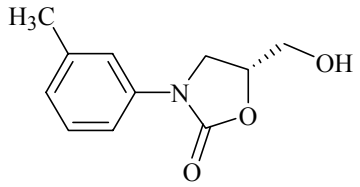

23

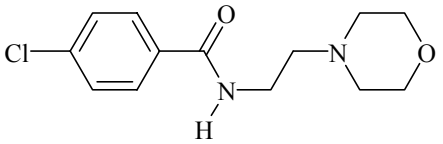

24

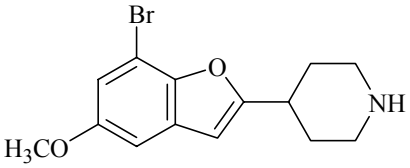

242

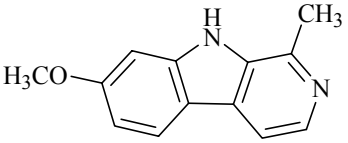

243

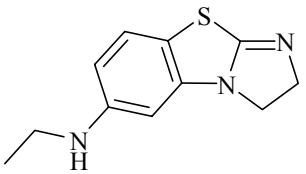

244

Medvedev *et al.* reported SAR studies on indole (**245**) and isatin (**246**) analogues with MAO inhibitory properties. Their initial work led to the conclusion that the dimensions of MAO-A and MAO-B inhibitors differ. The dimensions determined were 11.5x5.6x1.8 Å for MAO-A and 8.5x.5.1x1.8 Å for MAO-B indicating that the inhibitor binding site of MAO-B is smaller than MAO-A.[221] Based upon their more detailed analyses using CoMFA,[222] these authors proposed that steric and electrostatic factors contributed equally to the inhibitory properties of the indole derivatives. Although generated CoMFA maps for MAO-A and MAO-B showed common regions, the active sites of the enzymes were different.

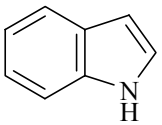

245

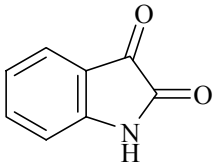

246

The same research group proposed a narrow and long active site cavity for MAO-A and a short and broader cavity for MAO-B based on their analyses of flexible

---

[221] Medvedev, A.E., Ivanov, A.S., Kamyshaskaya, N.S., Kirkel, A.Z., Moskvitina, T.A., Gorkin, V.Z., Li, N.Y., Marshakov, V.Y. (1995) Interaction of indole derivatives with monoamine oxidase A and B. Studies on the structure-inhibitory activity relationship. *Biochem. Mol. Biol. Internat.* **36**, 113-122.

[222] Medvedev, A.E., Ivanov, A.S., Veselovsky, A.V., Skvortsov, V.S., Archakov, A.I. (1996) QSAR analysis of indole analogues a monoamine oxidase inhibitors *J. Chem. Inf. Comput. Sci.* **36**, 664-671.

and rigid pyrazinocarbazole (**247**) derivatives.[223] The importance of steric and electrostatic components, specially at the 5 position of indolyl moiety, was confirmed by CoMFA analysis independenly by the research group of Pardo.[224]

CoMFA analyses of a series of coumarin (**248**) derivatives, which showed selective MAO-B inhibitory properties, demonstrated the importance of lipophilic interactions. The results of these SAR studies indicated no contribution of electronic properties on MAO-B inhibition.[225]

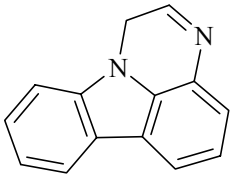

247

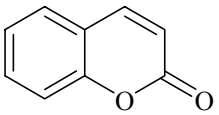

248

5.1.2. Modeling of MAO Active Site Based on the Structure of Tetrahydropyridinyl Derivatives as Substrates

Although the analyses of the structural features of MAO inhibitors are useful in developing pharmacophore models to facilitate the design of potent and specific MAO inhibitors of the A and B forms of the enzyme, they do not provide reliable information on the topology of MAO active sites. The limited value of these approaches is mainly due to the possibility of alternate binding modes. A potentially more informative approach is the utilization of substrate molecules as probes to explore the active sites of MAO-A and MAO-B.

One of the most widely studied classes of compounds are the tetrahydropyridinyl derivatives, the study of which emerged after the discovery of MPTP as a proneurotoxin.

---

[223] Tikhonova, O.V., Veselovsky, A.V., Medvedev, A.E., Ivanov, A.S. (2000) Models of monoamine oxidase A and B active sites obtained by using 3D QSAR with CoMFA *Molecular Simulation* **24**, 379-389.
[224] Moron, J.A., Campillo, M., Perez, V., Unzeta, M., Pardo, L. (2000) Molecular determinants of MAO selectivity in a series of indolylmethylamine derivatives: biological activities, 3D-QSAR/CoMFA analysis, and computational simulation of ligand recognition. *J. Med. Chem.* **43**, 1684-1691.
[225] Gnerre, C., Catto, M., Leonetti, F., Weber, P., Carrupt, P.A., Altomare, C., Carotti, A., Testa, B. (2000) Inhibition of monoamine oxidases by functionalized coumarin derivatives: biological activities, QSARs, and 3D-QSARs. *J. Med. Chem.* **43**, 4747-4758.

Studies on MPTP derivatives have revealed critical information on the three dimensional structures of the MAO active sites. The conformation of these molecules is partially constrained with only a few rotatable bonds. The two electron oxidation catalyzed by MAO is known to take place only on the allylic α-carbon of the tetrahydropyridinyl moiety. The presence of the tetrahydropyridinyl moiety, which is common to all MPTP analogs, further simplifies the construction of active sites models by dictating the alignment of the nitrogen-carbon bond undergoing oxidation

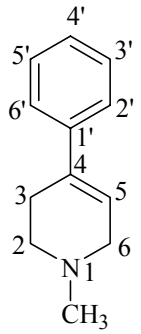

1

Studies on MPTP derivatives showed that substituents were only tolerated at the C-4 and N-1 positions of the THP ring.[226,227] Substrate properties were enhanced when the groups introduced at the C-4 position had lipophilic character.[228,229] Although both flexible and rigid substituents can be accommodated at C-4, bulkier groups are tolerated better by the MAO-A active site than the MAO-B active site.[230,231] The size of the N-1

---

[226] Fries, D.S., Vries, J., Hazelhoff, B., Horn, A.S. (1986) Synthesis and toxicity toward nigrostriatal dopamine neurons of 1-methyl-4-phenyl-1,2,3,6-tetrahydropyridine (MPTP) analogues. *J. Med. Chem.* **29**, 424-427.

[227] Maret, G., Tayar, N., Carrupt, P.-A., Testa, B., Jenner, P., Bairds, M. (1990) Toxication of MPTP (1-methyl-4-phenyl-1,2,3,6-tetrahydropyridine) and analogs by monoamine oxidase. *Biochem. Pharmacol.* **40**, 783-792.

[228] Altomare, C., Carrupt, P.-A., Gaillard, P., Tayar, N.E., Testa, B., Carotti, A. (1992) Quantitative structure-metabolism relationship analyses of MAO-mediated toxication by 1-methyl-4-phenyl-1,2,3,6-tetrahydropyridine and analogues. *Chem. Res. Toxicol.* **5**, 366-375.

[229] Efange, S.M.N., Boudreau, R.J. (1991) Molecular determinants in the bioactivation of the dopaminergic neurotoxin, N-methyl-4-phenyl-1,2,3,6-tetrahydropyridine (MPTP) *J. Comp. Aided Mol. Des.* **5**, 405-417.

[230] Efange, S.M.N., Michelson, R.H., Tan, A.K., Krueger, M.J., Singer, T.P. (1993) Molecular size and flexibility as determinants of selectivity in the oxidation of N-methyl-4-phenyl-1,2,3,6-tetrahydropyirdineanalogs by monoamine oxidase A and B. *J. Med. Chem.* **36**, 2178-2183.

[231] Tipton, K.F., Singer, T.P. (1993) Advances in our understanding of the mechanisms of the neurotoxicity of MPTP and related compounds. *J. Neurochem.* **61**, 1191-1206.

substituent is also critical for substrate properties. Presence of larger substituents than methyl at N-1 decreases the substrate properties.[232] However, the replacement of the methyl group with a hydrogen diminishes the substrate properties.[233] When small substituents are introduced at the para position of the C-4-phenyl ring, MAO-A substrate properties decrease whereas these compounds still show good MAO-B substrate properties. On the basis of this information an optimum distance of 10-12 Å for MAO-B substrates was suggested for the length of the main axis (N-1-C-4-C-1'-C-4') of the molecule.[234] This led to the proposal that the substrate binding cavity is slightly shorter in MAO-A than MAO-B.

5.1.3. Crystal Structure of MAO-B

The x-ray crystal structure at a resolution of 3Å of recombinant human liver MAO-B expressed in *Pichia pastoris*[235] was reported by the Edmondson laboratory in January, 2002.[236] The enzyme had been inactivated with the mechanism-based inactivator pargyline and existed as a homodimer. The flavin cofactor is attached to the cysteine 397 residue and the inactivator pargyline is covalently bound to the N5 nitrogen of the flavin. Recently the crystal structure of MAO-B at a resolution of 1.7 Å was also reported by Edmondson's group.[237,238] In these crystals the active site is occupied by a reversible inhibitor isatin (**246**).

The active site was shown to consist of an "entrance cavity" with a volume of 290 $Å^3$ and a "substrate binding" cavity with a larger volume of 420 $Å^3$. Four residues,

---

[232] Brossi, A. (1985) Further exploration of unnatural alkoloids. *J. Nat Prod.* **48**, 878-893.
[233] Kalgutkar, A.S., Dalvie, D.K., Castagnoli, N., Jr., Taylor, T.J. (2001) Interactions of nitrogen-containing xenobiotics with monoamine oxidase (MAO) isozymes A and B: SAR studies on MAO substrates and inhibitors. *Chem. Res. Toxicol.* **14**, 1139-62.
[234] Mabic, S., Castagnoli, N., Jr. (1996) Assesment of structural requirements for the monoamine oxidase-B-catalyzed oxidation of 1,4-disubstituted-1,2,3,6-tetrahydropyridine derivatives related to the neurotoxin 1-methyl-4-phenyl-1,2,3,6-tetrahydropyridine. *J. Med. Chem.* **39**, 3694-3700.
[235] Newton-Vinson, P., Hubalek, F., Edmondson, D.E. (2000) High level expression of human liver monoamine oxidase B in *Pichia pastoris*. *Protein Exp. Purif.* **20**, 334-345.
[236] Binda, C., Newton-Vinson, P., Hubalek, F., Edmondson, D.E., Mattevi, A. (2002) Structure of human monoamine oxidase B, a drug target for the treatment of neurological disorders. *Nat. Struct. Biol.* **9**, 22-26.
[237] Binda, C., Li, M., Hubalek, F., Restelli, N., Edmondson, D.E., Mattevi, A. (2003) Insights into the mode of inhibition of human mitochondrial monoamine oxidase B from high-resolution crystal structure. *Proc. Natl. Acad. Sci. U.S.A.* **100**, 9750-9755.
[238] Hubalek, F., Binda, C., Li, M., Mattevi, A., Edmondson, D.E. (2003) Polystyrene microbridges used in sitting-drop crystallization release 1,4-diphenyl-2-butene, a novel inhibitor of human MAO B. *Acta Crystallogr. D Biol. Crystallogr.* **59**, 1874-1876.

Leu 171, Tyr 326, Ile 199, Phe 168 serve as a gate between the two cavities. These residues, together with Phe 343, Tyr 398, Cys 172, Tyr 60, Tyr 435, Gln 206 and Tyr 188, constitute the substrate cavity as shown in Figure 56.[239] All of the active site residues are conserved in MAO-A, except for three of the residues that separate the entrance cavity from the substrate cavity in MAO-B, Leu 171, Tyr 326, Ile 199. These residues are replaced with Ile 180, Ile 335, and Phe 208, respectively, in MAO-A.

Figure 56. The stereo view of the residues defining the active site of human MAO-B.

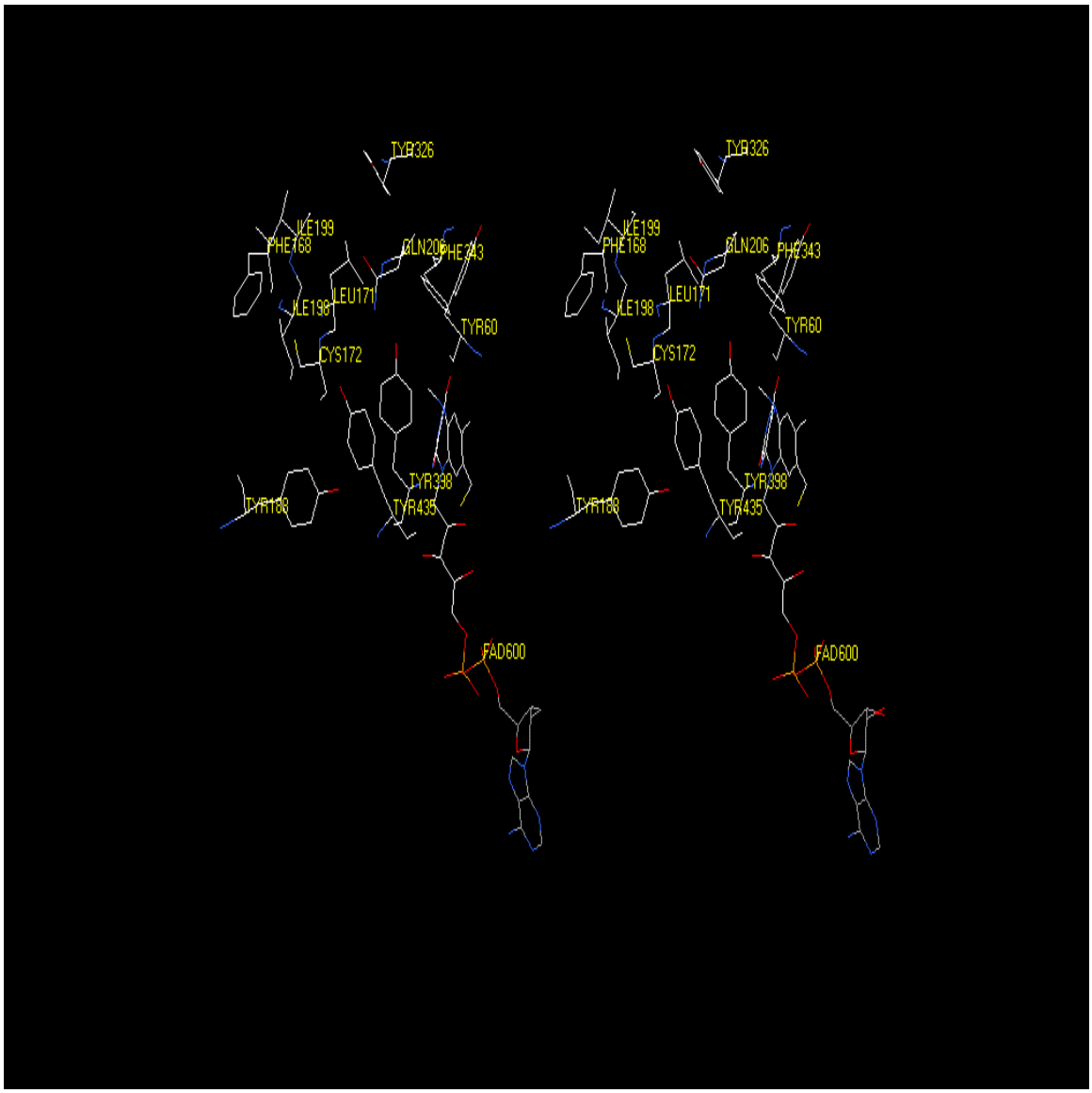

239 Figure 1 is generated from the pdb file of the x-ray crystal structure of MAO-B (1GOS) available from the Protein Data Bank at www.rcsb.org/pdb/ using Swiss-PdbViewer.

In an attempt to provide a better understanding of the previously observed MAO-B substrate and inhibitor properties of the nitroindazolyl "prodrugs", x-ray crystal structure of MAO-B was utilized in the docking studies. These studies will be presented in Section 5.4. A summary of the previous studies on the interaction of nitroindazolyl "prodrugs" with MAO-B will be given, first.

5.2. Previous Studies on the MAO-B Substrate Properties of Nitroindazolyl Prodrugs

Our previous synthetic efforts had led to the preparation of the 1*H*- "prodrugs" of 5- and 6-NI (**45** and **46**, respectively) and the 2*H*- "prodrug" of 7-NI (**28**). Substrate properties of these prodrugs have been investigated by incubating the "prodrugs" in the presence of baboon liver mitochondria which express only the B form of MAO.[240] The incubation mixtures were analyzed by HPLC-DA after sedimenting the protein upon centrifugation.

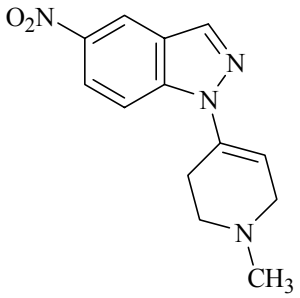

45

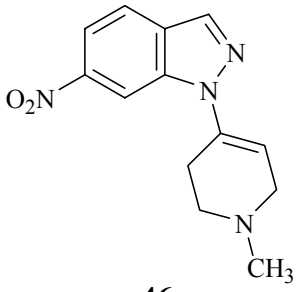

46

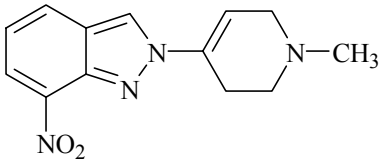

28

No metabolite formation was observed for the 2*H*- 7-NI "prodrug" **28** in the presence of MAO-B. However, HPLC tracings showed the formation of two metabolite peaks for both 1*H*- "prodrugs" **45** and **46** accompanied by a decrease in the intensities of the peaks corresponding to the starting materials. Upon comparison of the retention times and the UV spectra, these metabolite peaks were identified as the corresponding pyridinium species **49**, **50** and the parent indazoles **42** and **43**, respectively. On the basis of the HPLC tracings, the pyridinium species seemed to be the major metabolites.

---

[240] Reference 51.

Scheme 95. Metabolism of nitroindazolyl "prodrugs" by MAO-B.

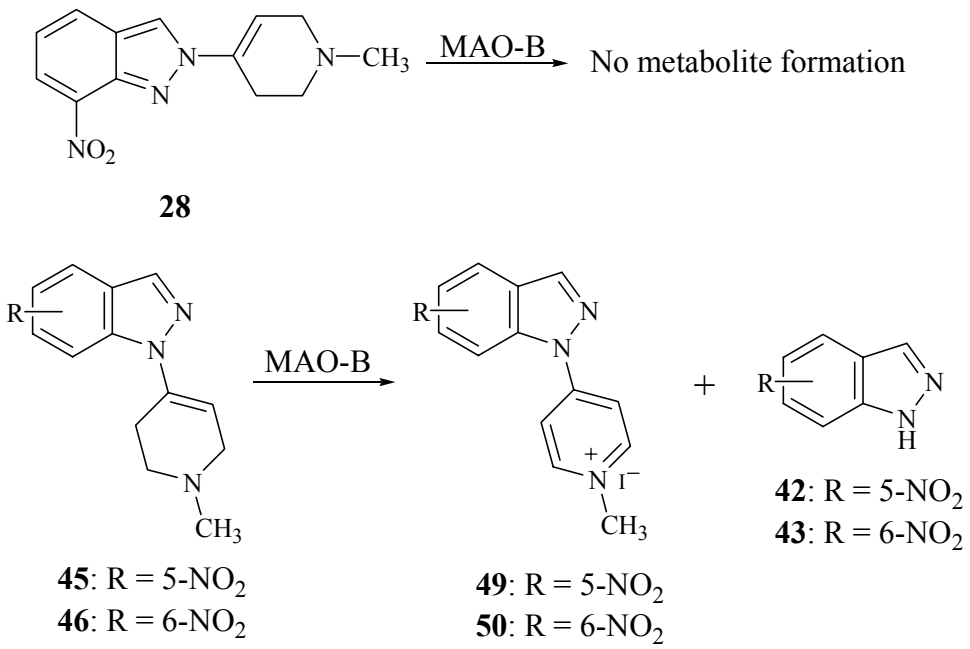

The pathways leading to the formation of metabolites **49**, **50**, **42** and **43** are described in Scheme 96. The MAO-B catalyzed two electron α-carbon oxidation of the "prodrugs" **45** and **46** results in the formation of the corresponding dihydropyridinium derivatives **249** and **250**, respectively. Further oxidation of these dihydropyridinium derivatives will lead to formation of the pyridinium metabolites **49** and **50** which were shown to be stable under aqueous conditions by obtaining the ^{1}H NMR spectra in D_2O.[241] Alternatively, hydrolysis of the dihydropyridinium derivatives **249** and **250** followed by cleavage will give the parent indazoles **42**, **43** and aminoenone **32**.

[241] Reference 1.

Scheme 96. MAO-B catalyzed formation of nitroindazolylpyridinium derivatives 49, 50 and parent nitroindazoles 42 and 43.

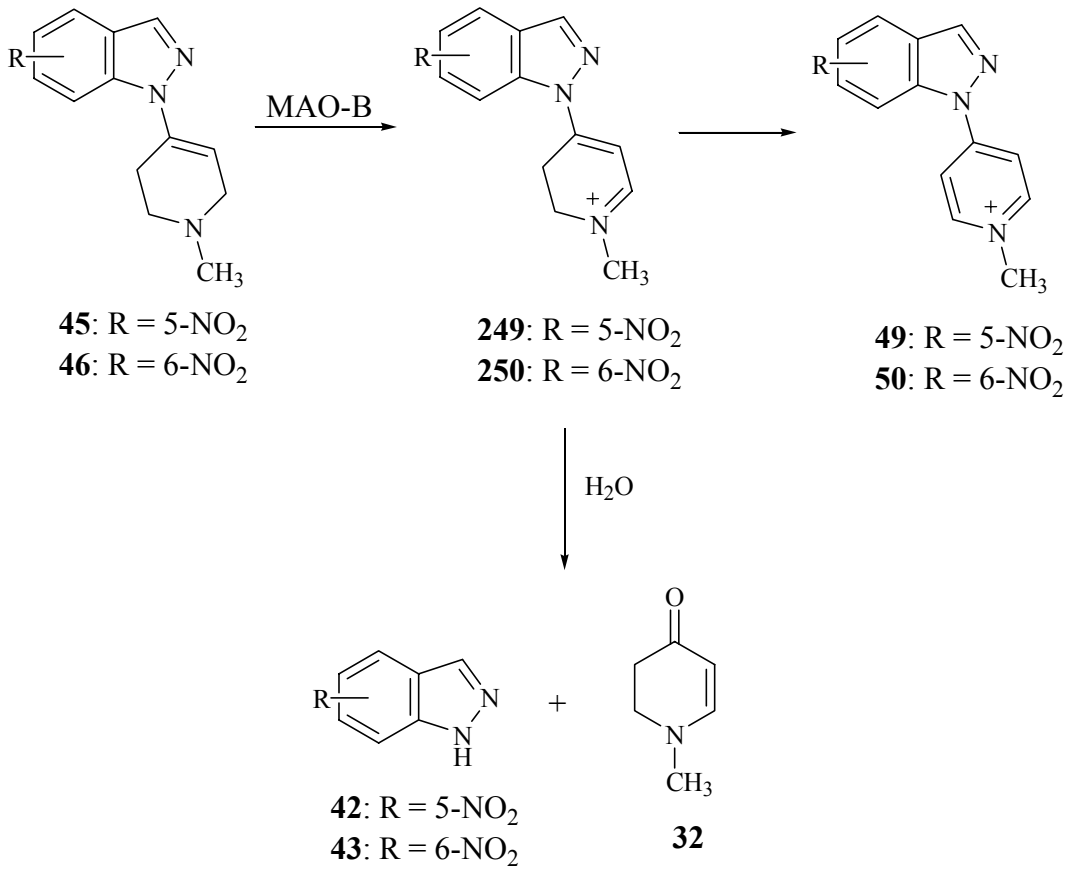

MAO-B substrate properties of the 1*H*-prodrugs **45** and **46** as well as the non-substrate property of the 2*H*-prodrug **28** were in agreement with the previously investigated isomeric protioindazolyltetrahydropyridinyl derivatives **251** and **252** and the benztriazolyltetrahydropyridinyl derivatives **253** and **254**. The 1*H*-isomers **251** and **253** have been reported to be MAO-B substrates whereas the 2*H*-isomers **252** and **254** did not display any MAO-B substrate properties.[242]

[242] Reference 104.

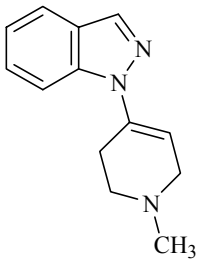

251

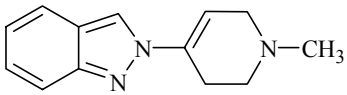

252

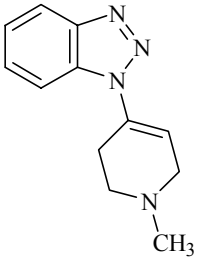

253

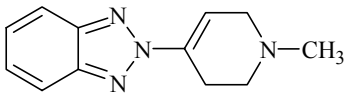

254

An MAO-B active site model suggested that 1*H*-isomers **45** and **46** should fit well into the active site of MAO-B.[243] However, the 2*H*-isomer **28** was unlikely to fit into the active site mainly due to the length of the molecule along its main axis compared to the length of the active site estimated on the basis of the model.[244] Interestingly, although the 2*H*-7NI prodrug **28** was not an MAO-B substrate it was shown to be an MAO-B inhibitor. This outcome was rationalized by a proposed alternate conformation of **28** in the active site leading to the inhibition of the enzyme.

Additional studies showed the time dependent loss of enzyme activity in the presence of "prodrug" **46**. It was suggested that the loss of enzyme activity may be due to the release of the parent compound, 5-NI (**42**), following the bioactivation of the "prodrug" by MAO-B. However, it was also possible that the formation of pyridinium metabolite may be responsible for the time dependent inhibition of the enzyme.

5.3. Studies on the MAO-A Substrate Properties of Nitroindazolyl Prodrugs

5.3.1. Studies on the 2*H*-7-NI Prodrug

Based on the active site model of MAO-B, it was suggested that the steric factors prevent the 2*H*-7NI prodrug **28** from assuming a favorable conformation in the active site. Since the MAO-A active site was known to tolerate larger substrates, it was decided to investigate MAO-A substrate properties of **28**. Human placenta was used as the

---

[243] Palmer, S.L., Mabic, S., Castagnoli, N., Jr. (1997) Probing the active sites of monoamine oxidase A and B with 1,4-disubstituted tetrahydropyridine substrates and inactivators. *J. Med. Chem.* **40**, 1982-1989.
[244] For figures describing the active site model see Reference 1 pages 115 and 118.

enzyme source. This tissue expresses only the A form of the enzyme.[245] Compound **28** (40 μM final concentration) was incubated in the presence of human placenta (0.3 mg/mL final protein concentration), the incubations were stopped by adding acetonitrile and supernatants from the incubation mixtures were analyzed by HPLC-DA after sedimenting the protein via centrifugation. The results are shown in Figure 57.

[245] O'Carroll, A.M., Anderson, M.C., Tobbia, I., Phillips, J.P., Tipton, K.F. (1989) Determination of the absolute concentrations of monoamine oxidase A and B in human tissues. *Biochem. Pharmacol*. **38**, 901-905.

Figure 57. HPLC-DA tracings obtained for the incubation mixtures containing the 2*H*-7-NI prodrug 28 and human placenta as the MAO-A source.

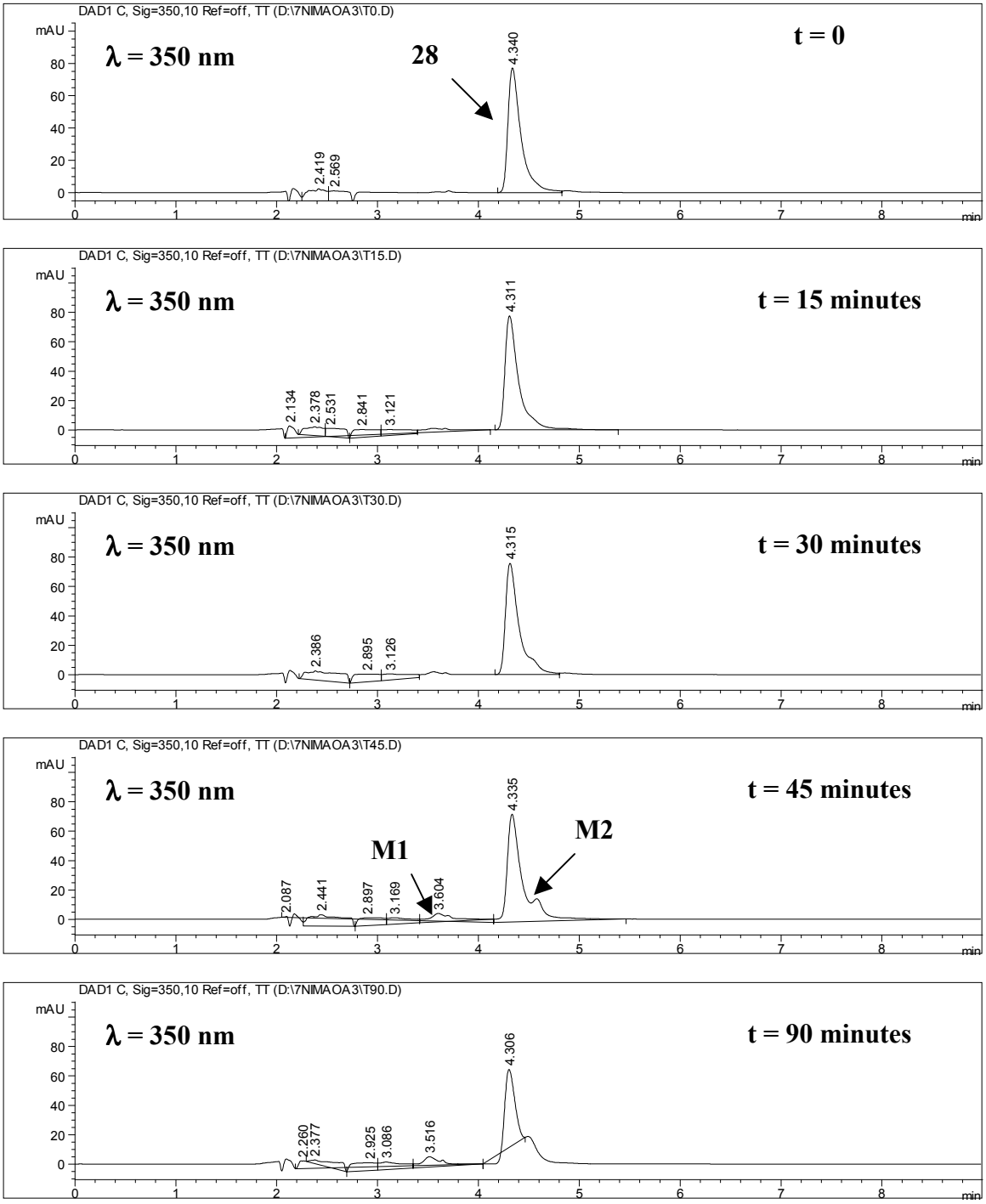

The intensity of the peak corresponding to compound **28** decreased slowly over time and two peaks (**M1** and **M2**) with low intensity appeared with retention times 3.6

and 4.6 minutes. Based on its retention time, the first metabolite (**M1**) was proposed to be the corresponding nitroindazolylpyridinium **54**. Indeed, the UV spectrum of **M1** (t_R = 3.4 minutes) was essentially identical to the UV spectrum of synthetic 4-(2*H*-7-nitroindazolyl)-1-methylpyridinium iodide (**54**) supporting this proposal. (Fig. 58).

Figure 58. UV spectrum of metabolite M1 (a) and UV spectrum of synthetic 54 (b).

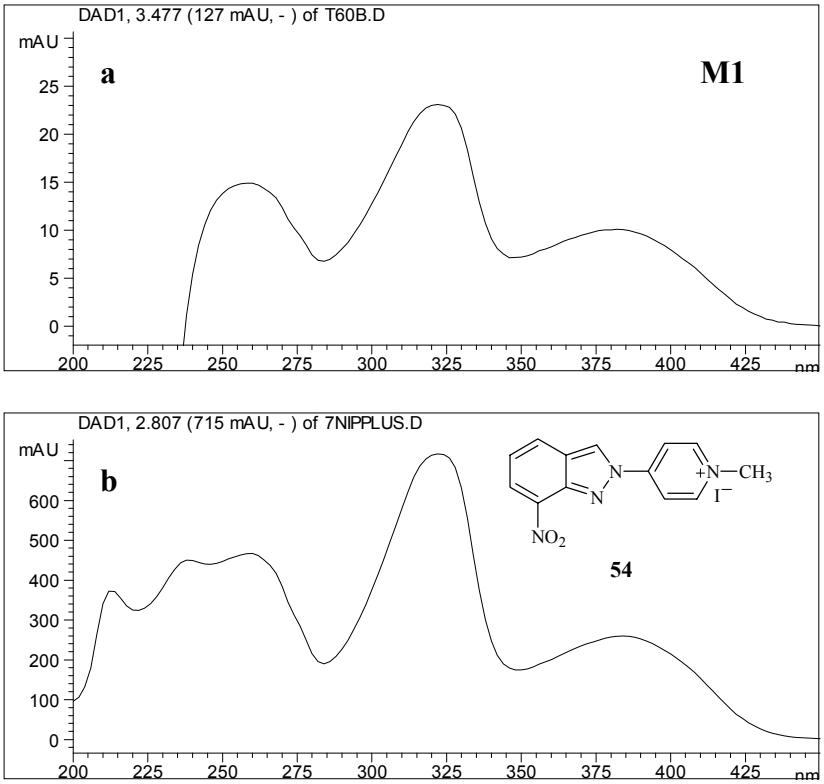

Based on its retention time of 4.6 minutes, it is likely that the second metabolite (**M2**) is the parent 7-nitroindazole. The comparison of the UV spectrum of **M2** with synthetic 7-nitroindazole supported this assignment (Fig. 59).

Figure 59. UV spectrum of metabolite M2 (a) and UV spectrum of synthetic 7-NI [(25) b].

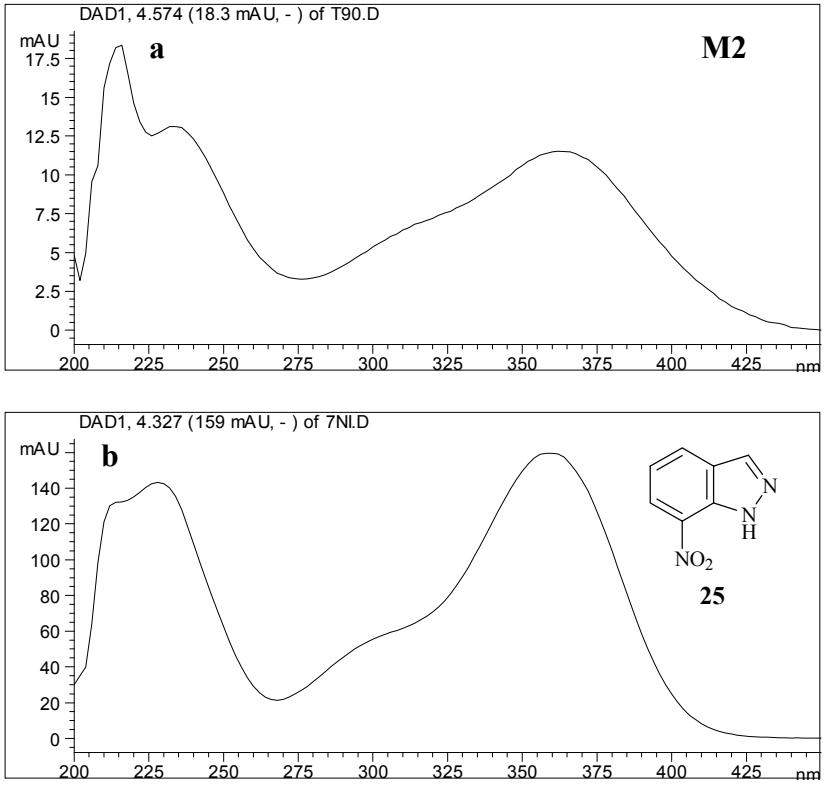

Metabolite formation was observed for 2*H*-7-NI prodrug **28** in the presence of MAO-A. However, the extent of conversion was very limited suggesting that compound **28** is a poor MAO-A substrate. It is also possible that the inhibition of the enzyme by the metabolites **25** and **54** results in the time dependent loss of enzyme activity which will mask the substrate properties of the 2*H*-7-NI prodrug. Although substrate turnover was shown to take place slowly, the release of 7-NI in addition to the pyridinium metabolite was encouraging for the applicability of the "prodrug" concept.

5.3.2. Studies on the 1*H*-5-NI and 1*H*-6-NI Prodrugs

The 1*H*-prodrugs of 5- and 6-NI **45** and **46** were also tested for their MAO-A substrate properties. The final substrate and protein concentrations were 40 μM and 0.15 mg/mL, respectively. HPLC-DA tracings obtained for MAO-A incubation of **45** and **46** are shown in Figures 60 and 61.

Figure 60. HPLC-DA tracings for the incubation of the 1*H*-5-NI prodrug 45 with human placental MAO-A.

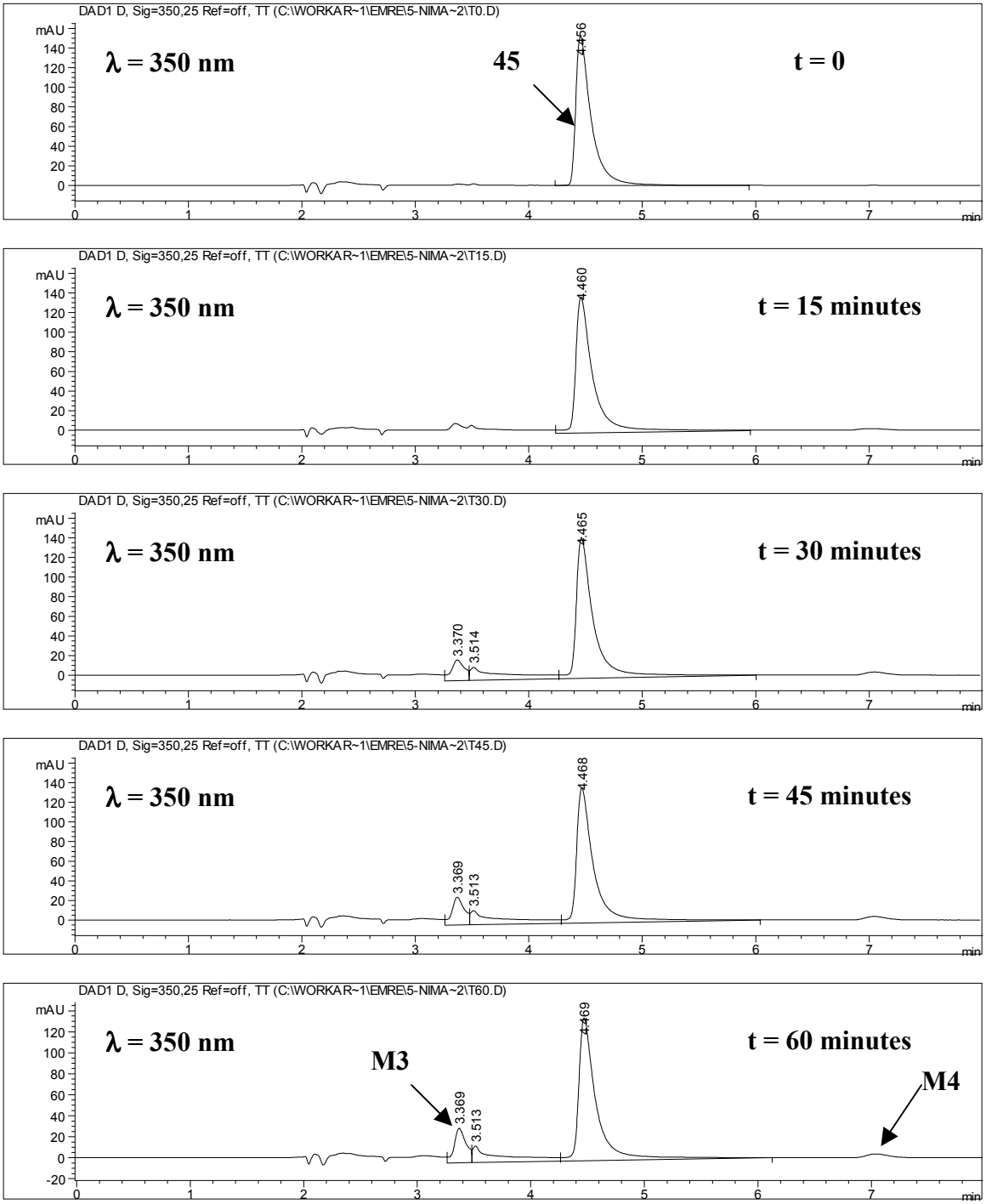

Figure 61. HPLC-DA tracings for the incubation of the 1*H*-6-NI prodrug 46 with human placental MAO-A.

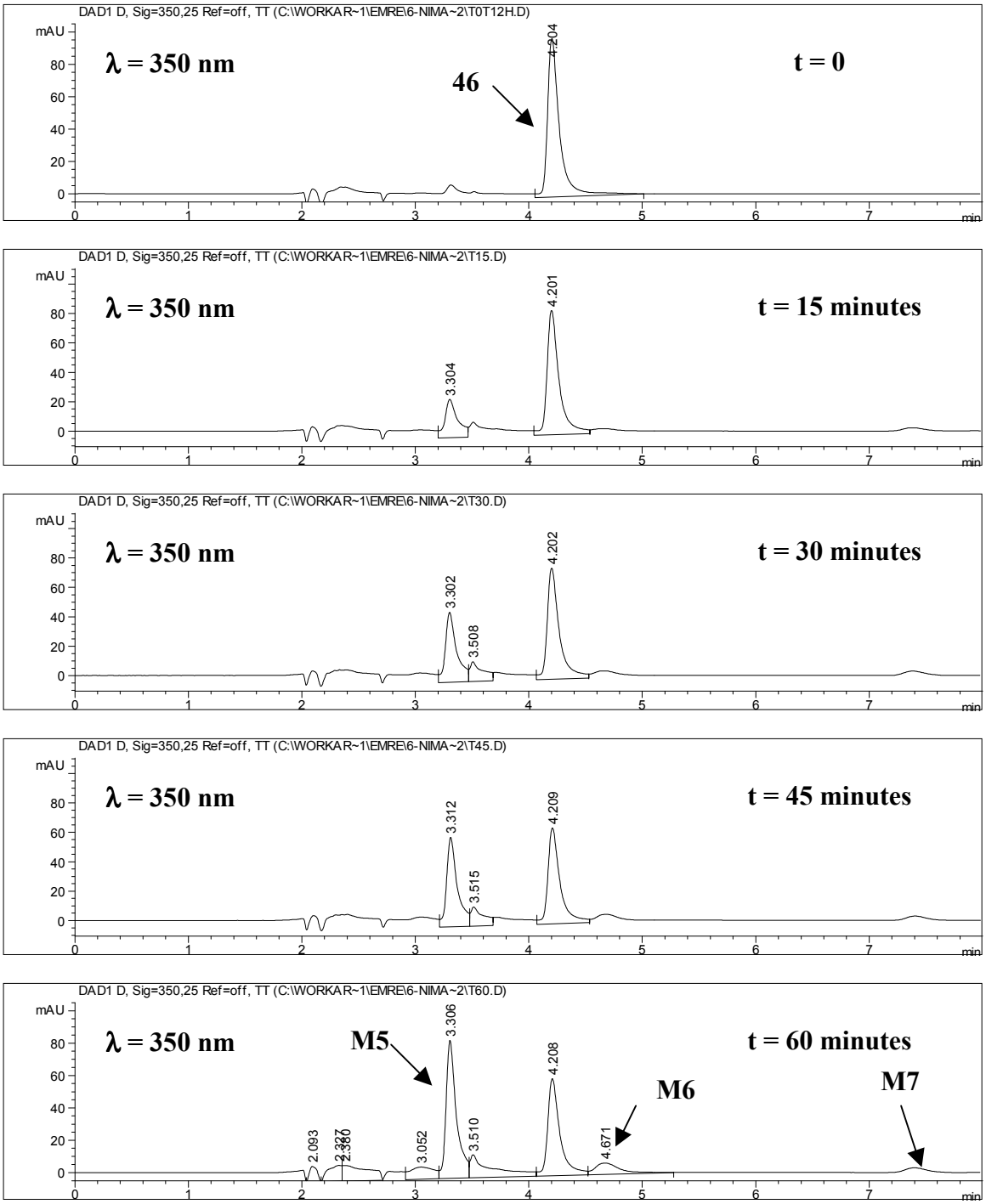

In the case of the 5-NI "prodrug" **45**, the intensity of the peak corresponding to the substrate decreased only slightly (approximately 5% based on the height of the

substrate peak) whereas the extent of substrate turnover was higher for the 6-NI "prodrug" (approximately 30% based on the height of the substrate peak). HPLC-DA tracings for both prodrugs were similar to the previously obtained results for the MAO-B incubations[246] suggesting the formation of the same metabolites. Comparison of the UV spectra of the metabolites with the synthetic standards showed that **M3** and **M5** have identical UV spectra with the corresponding pyridinium derivatives **49** and **50** (Figs. 62 and 63). The UV spectrum of **M6** was identical with the UV spectrum of parent 6-nitroindazole [(**43**) Fig. 64]. The expected formation of 5-NI (**42**) from the 5-NI "prodrug" was not detected by HPLC-DA, possibly reflecting limited substrate turnover.

Figure 62. UV spectra of metabolite M3 (a) and synthetic 4-(1*H*-5-nitroindazolyl)-1-methylpyridinium iodide[(49) b].

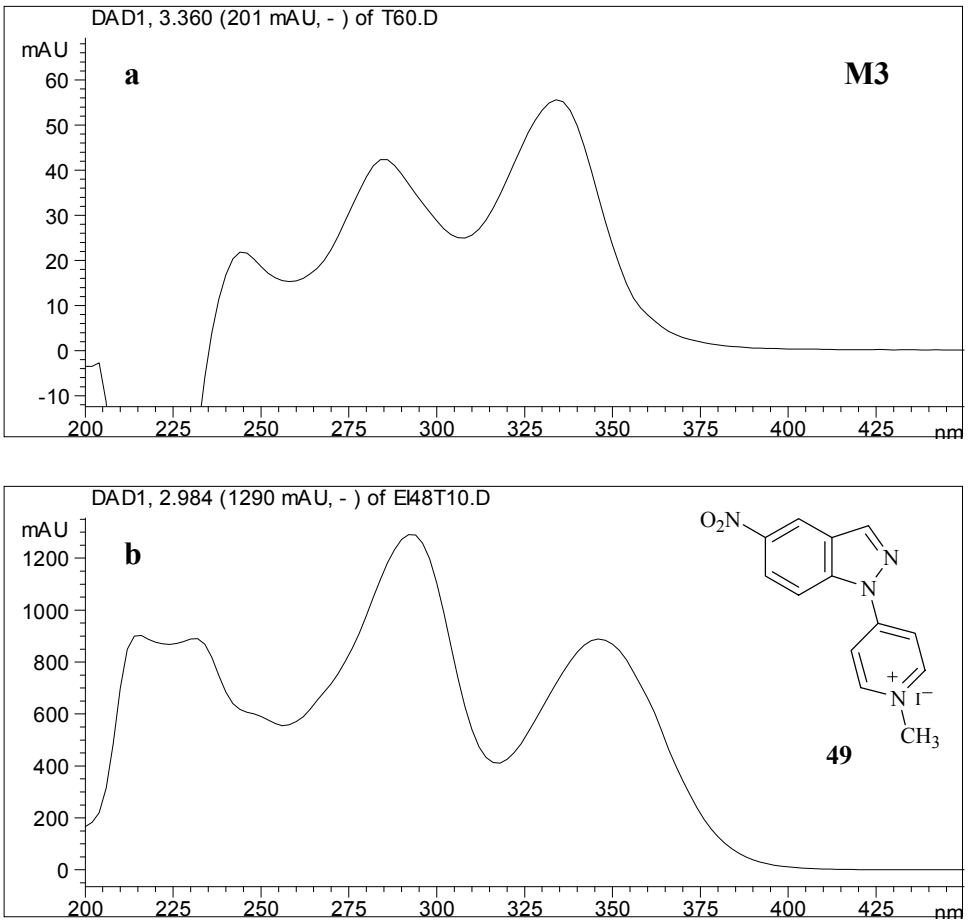

[246] See Reference 1, pages 121-122.

Figure 63. UV spectra of metabolite M5 (a) and synthetic 4-(1*H*-6-nitroindazolyl)-1-methylpyridinium iodide[(50) b].

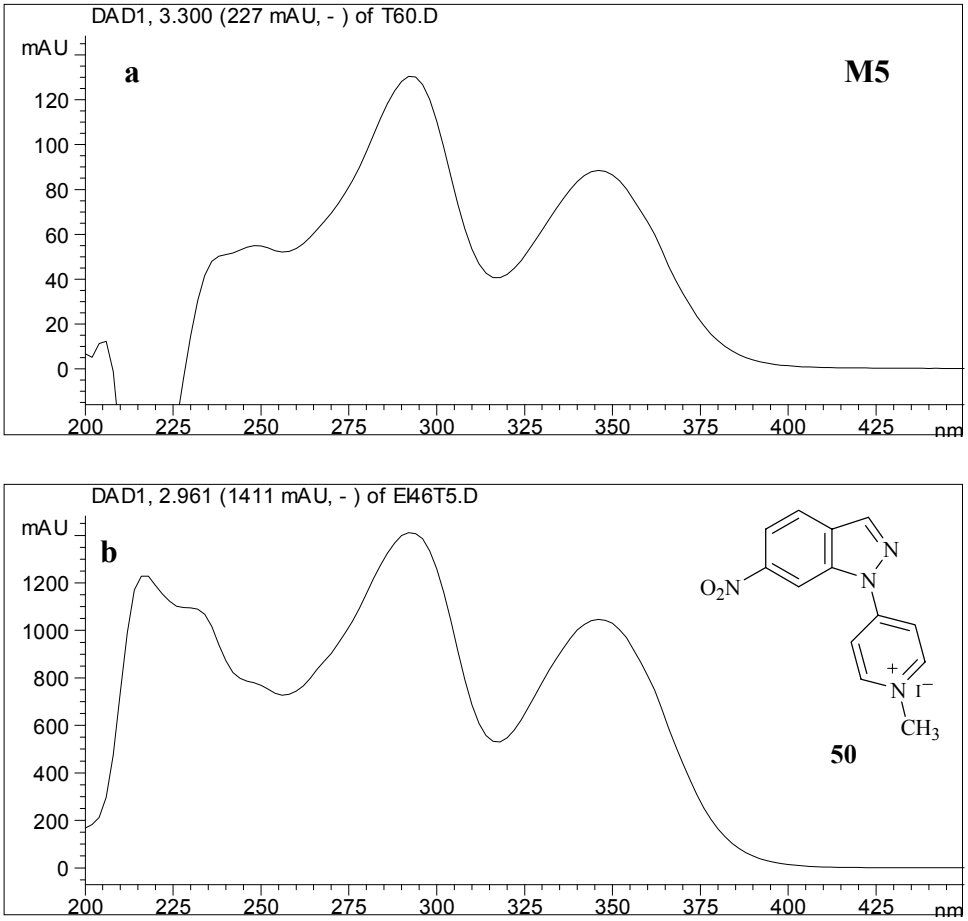

Figure 64. UV spectra of metabolite M6 (a) and synthetic 6-nitroindazole [(43) b].

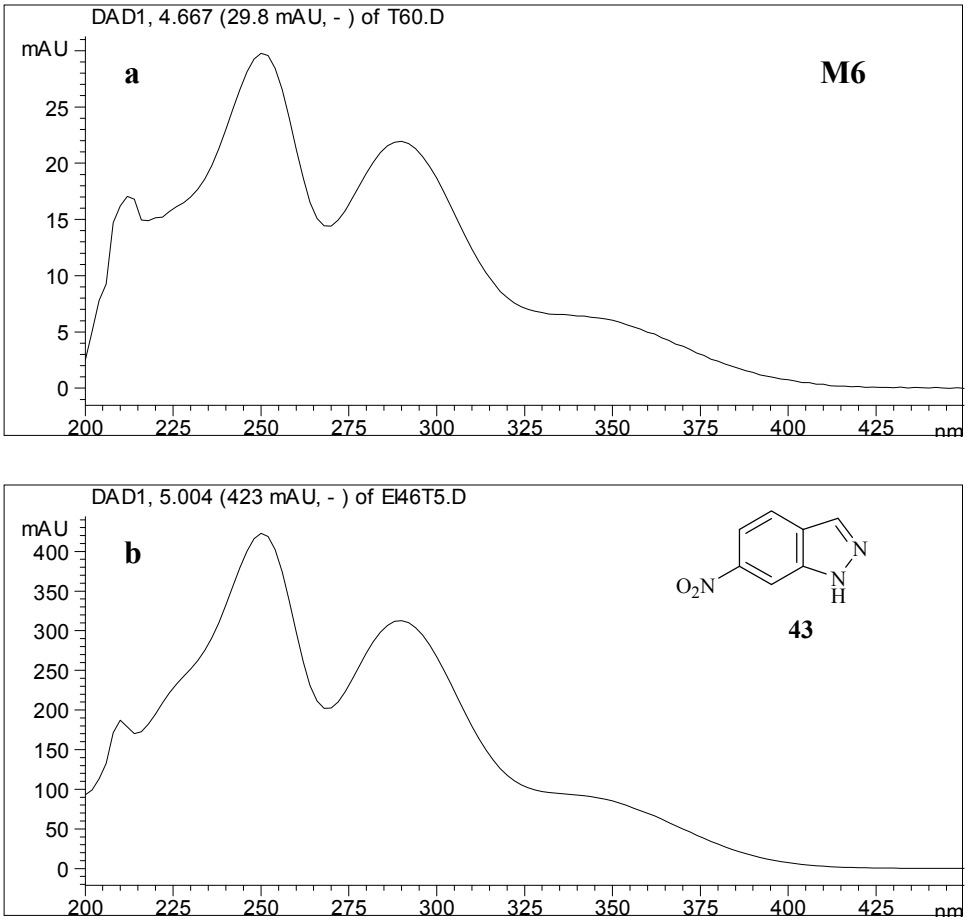

In order to investigate further the structure of the metabolites, LC-MS was utilized. Mass spectral analysis is expected to provide supporting evidence for the characterization of metabolites **M3**, **M5** and **M6**. Also, it was hoped that unknown metabolites **M4** and **M7** might be identified based on the mass spectral data. The supernatant from the 1*H*-5-NI prodrug incubation mixture was analyzed by LC-MS using APCI as the ionization source. The TIC tracing and the mass spectra obtained for substrate and metabolite peaks are shown in Figure 65.

Figure 65. LC-APCIMS analysis of 1*H*-5-NI prodrug MAO-A incubation mixture (t=1 hour).

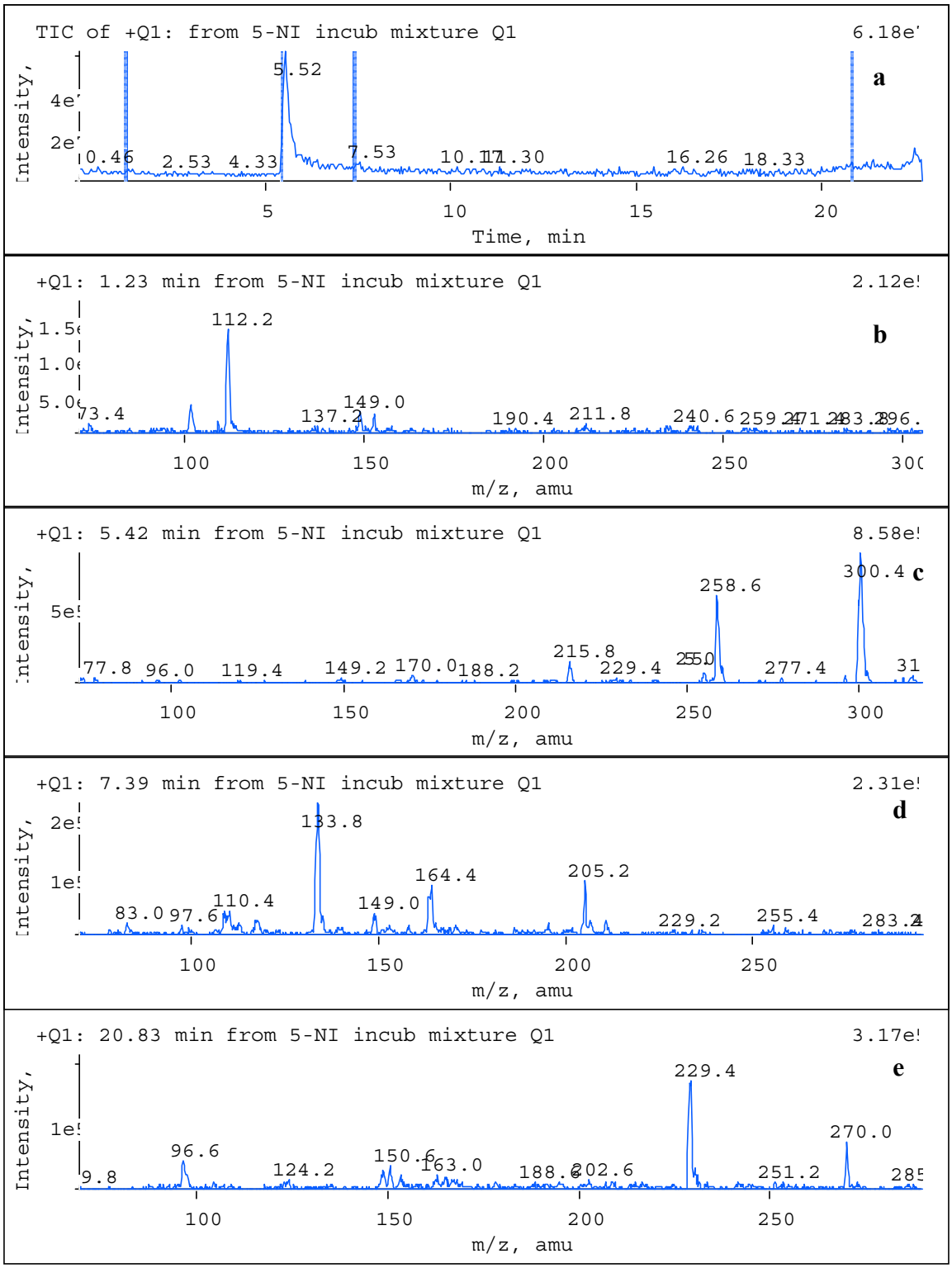

LC-MS analysis shows that metabolite **M3**, previously identified as 4-(1*H*-5-nitroindazolyl)-1-methylpyridinium [(**49**), M^+ 255] via comparison with the synthetic standard, co-elutes with the substrate [(**45**), MH^+ 259, t_R = 5.5 minutes].[247] The MH^+ 300 peak is likely due to adduct formation between **45** and acetonitrile (Fig. 65c). Although it was not detected by HPLC-DA, LC-MS analysis shows the presence of parent 5-NI [(**42**), MH^+ 164) together with its acetonitrile adduct [MH^+ 205, (Fig. 65d)]. In addition to the previously observed metabolites, the mass spectrum obtained at 1.2 minutes revealed the presence of a molecule with MH^+ 112 which is consistent with the protonated form (**255**) of the aminoenone **32** (Scheme 97), the expected second-product of the cleavage reaction leading to the release of the parent 5-NI (Scheme 96 above).

Scheme 97. Protonation of aminoenone 32 under LC-MS conditions to give 4-hydroxy-1-methyldihydropyridinium (255).

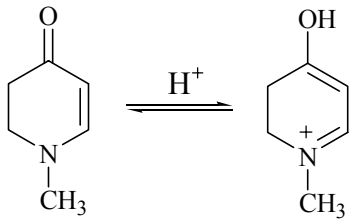

32 **255**

The mass spectrum obtained for metabolite **M4** with a retention time of 7.1 minutes in the HPLC-DA tracings (Fig. 60) showed MH^+ of 229 together with 270 which is proposed to be acetonitrile adduct (Fig. 65e). The loss of 30 amu from the substrate **45** (MH^+ 259) suggests the reduction of the nitro group in the incubation mixtures resulting in the formation of 5-aminotethrahydropyridine derivative **256** (Scheme 98).

[247] The difference in retention times between HPLC-DA and HPLC-MS analyses is due to the change in the mobile phase. See Experimental for details.

Scheme 98. Reduction of the nitro group coupled to α-carbon oxidation of the tetrahydropyridinyl moiety.

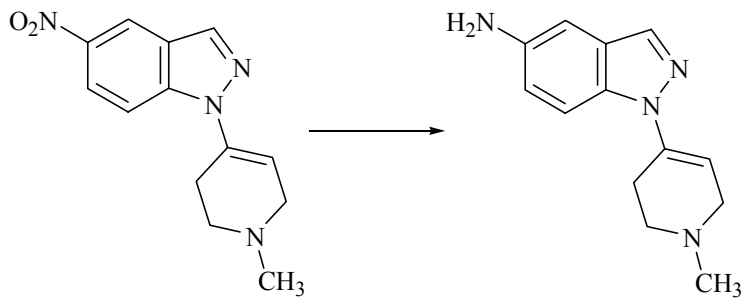

45 $MH^+ = 259$ **256** $MH^+ = 229$

The supernatant from the 1*H*-6-NI prodrug incubation mixture was also analyzed by LC-MS. The TIC tracing and the mass spectra obtained for substrate and metabolite peaks are shown in Figure 66.

Figure 66. LC-APCIMS analysis of 1*H*-6-NI prodrug MAO-A incubation mixture (t=1 hour).

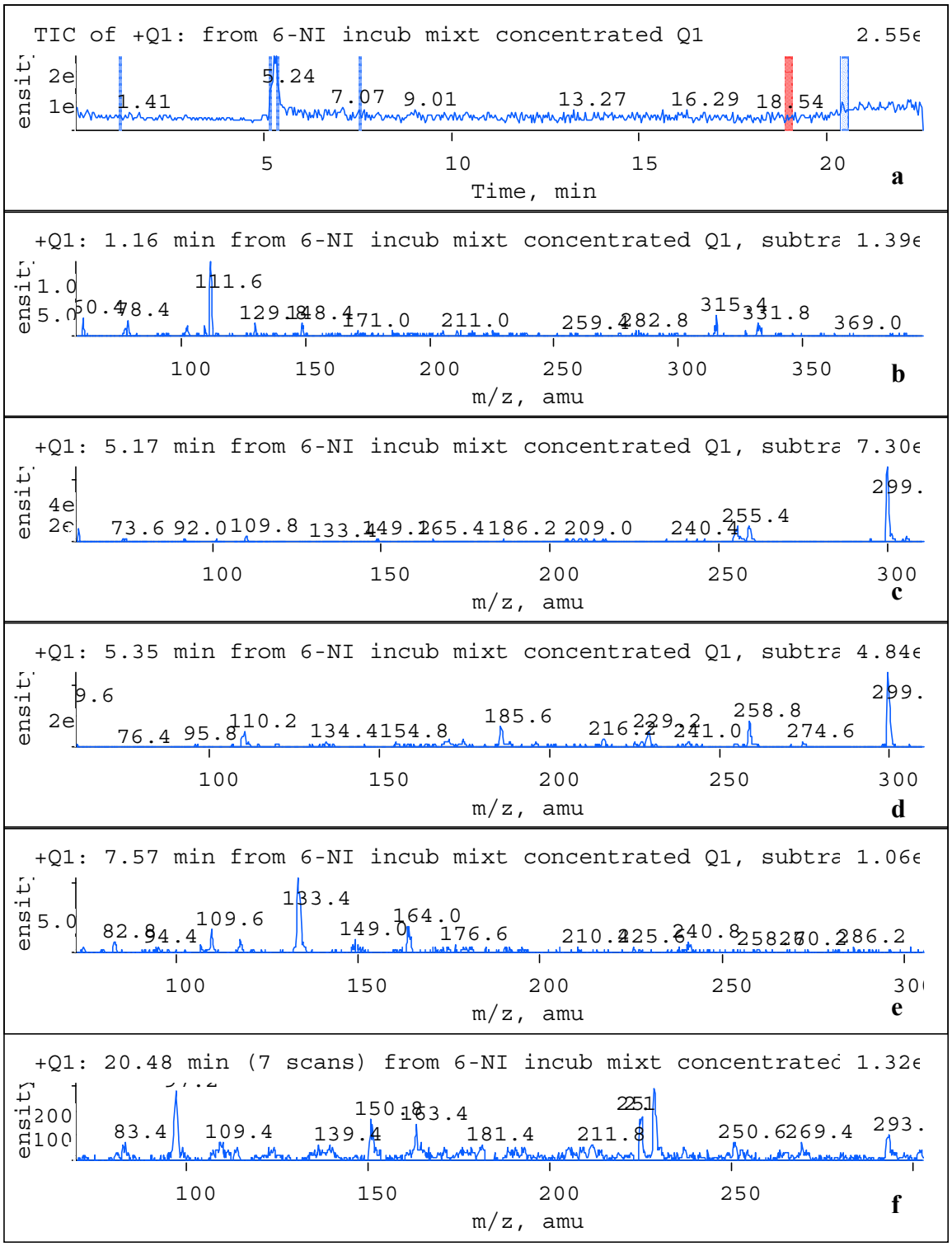

Results of the LC-MS analysis of the 1*H*-6-NI-prodrug incubation mixture were similar to the results obtained for the 1*H*-5-NI-prodrug. Although they are not separated, the pyridinium metabolite **50** [MH^+ 255, (Fig. 66c)] has a slightly earlier retention time than the substrate **46** [(MH^+ 259, (Fig. 66d)]. In addition to the cleavage products (**32** (Fig. 66a) and **43** (Fig. 66e), the MH^+ 229 peak was also present (Fig. 66f) which is proposed to be the aminotethradydrpyridine derivative **257**. This time, however, a second compound with MH^+ 225 that co-eluted with **257** was observed. The presence of this new peak can be rationalized by the oxidation of **257** by MAO-B following its formation to give **258** as shown in Scheme 99.

Scheme 99. Reduction of the nitro group of 46 followed by the oxidation of the tetrahydropyridinyl moiety to form 258.

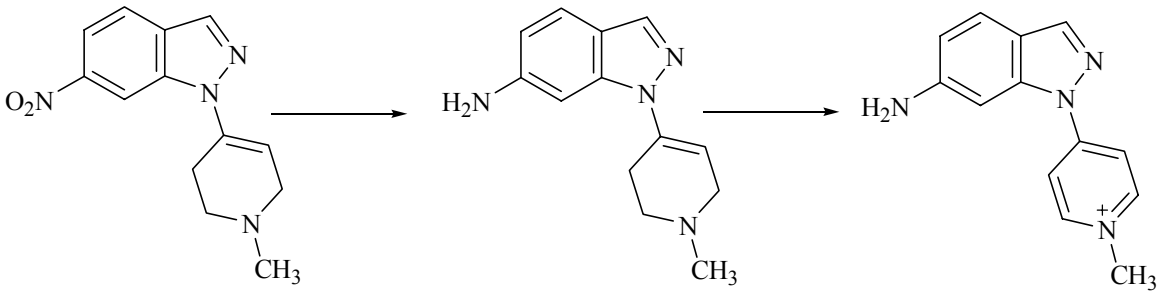

46 $MH^+ = 259$ **257** $MH^+ = 229$ **258** $M^+ = 225$

5.3.3. Summary of Preliminary Results Obtained from MAO-A Incubation of Nitroindazole "Prodrugs"

Substrate property studies showed that the 2*H*-7-NI "prodrug" as well as the 1*H*-5-NI and 1*H*-6-NI prodrugs are MAO-A substrates. The 1*H*-6-NI "prodrug" **46** displayed the largest extent of turnover whereas 2*H*-7-NI "prodrug" **28** and 1*H*-5-NI "prodrug" **45** displayed poor substrate properties relative to **46**. For all three "prodrugs", the release of the parent nitroindazole was observed together with the formation of the corresponding pyridinium metabolites. The LC-MS analyses carried out for "prodrugs" **45** and **46** provided further support for the structure of these two metabolites. Aminoenone **32** was detected by LC-MS analysis, formation of which is in agreement with the proposed

bioactivation pathway leading to the release of the parent nitroindazoles. Mass spectral data indicate the formation of aminotetrahydropyridinyl derivatives **256** and **257** via the reduction of the nitro group of **45** and **46**. This interesting transformation is poorly understood at this point. LC-MS analysis suggested that compound **257** undergoes oxidation to the corresponding pyridinium derivative **258**.

The release of parent nitroindazoles from the 1*H*-prodrugs **45** and **46** had been observed previously in MAO-B incubations. MAO catalyzed release of 7-NI from the corresponding prodrug **28** was observed for the first time. Although **28** appears to be a poor MAO-A substrate, the release of 7-NI was encouraging in relation to the applicability of the desired ”prodrug” approach to *in vivo* neuroprotection studies.

5.4. Docking Studies

Our previous results (Section 5.2) had shown that the 1*H*- “prodrugs” were MAO-B substrates whereas the 2*H*-7-NI-prodrug was an MAO-B inhibitor rather than a substrate. MAO-B substrate properties of the 1*H*- “prodrugs” had been rationalized[248] by their structural “fit” into the active site model developed previously.[249] In the case of the 2*H*-7-NI “prodrug”, this “fit” was not favored. Therefore, it is possible that 2*H*-7-NI assumes an alternative binding conformation resulting in the observed MAO-B inhibitory properties. With the availability of the x-ray crystal structure of MAO-B, it was decided to investigate further these preliminary analyses with the aid of docking studies. FlexiDock, which is an automated docking program with a genetic algorithm, [250] was utilized for the docking studies. The results of these preliminary docking studies will be presented. Since the x-ray crystal structure of MAO-A has not been solved up to this date, our docking studies will be limited to the active site of MAO-B.

5.4.1. Preparation of the Enzyme and the Ligands for Docking Studies

The coordinates of the x-ray crystal structure of MAO-B in complex with the reversible inhibitor isatin (**247**) were downloaded from the Brookhaven Protein Databank

---

[248] Reference 1, page 120.
[249] Reference 243.
[250] Judson, R., "Genetic Algorithms and Their Use in Chemistry" in Reviews in Computational Chemistry, Vol. 10, K.B. Lipkowitz and D.B. Boyd, eds., VCH Publishers, 1997.

in the protein data bank (PDB) file format and used for the docking studies. The PDB file was modified by deleting one of the subunits of the homodimeric structure and the water molecules. The ligands were constructed and minimized in SYBYL software. From the FlexiDock program, which is a part of the Biopolymer module of the SYBYL software,[251] the active site was defined relative to the coordinates of isatin. After defining the active site, isatin was removed. The atomic charges for the enzyme and the ligands were calculated and assigned. The rotatable bonds of the ligands were defined whereas the enzyme was kept rigid. After placing the ligand in the vicinity of the active site, the initial ligand/enzyme complex was submitted for the docking analysis and various binding conformations were automatically generated and their relative energies were obtained. Minimization of the resulting ligand/enzyme complexes was not attempted.

A detailed review by Mattevi's group on the x-ray crystal structures of various flavoenzymes reveals among other commonalities that the carbon atom undergoing oxidation is in almost all cases located at a highly conserved position at a distance of 3.5 Å from the N5 atom of the flavin cofactor.[252] Therefore, among the generated docking models, only those models which satisfy the above described criteria (carbon atom undergoing oxidation being close to the N5 atom of flavin) were considered for further evaluation.

5.4.2. Docking of the 1*H*-6-NI "Prodrug"

Among the generated ligand/enzyme complexes, two of the binding conformations had the α-carbon of the tetrahydropyridinyl ring placed towards the N5 atom of the flavin ring. The conformation with the lower energy of these two ligan/enzyme complexes is shown in Figure 67.

---

[251] Klotz, K.-N., Leung, E. Varani, K., Gessi, S. Merighi, S. Sybyl Molecular Modeling System, version 6.9. Tripos Inc., St. Louis, MO.

[252] Fraaije, M.W., Mattevi, A. (2000) Flavoenzymes: diverse catalysts with recurrent functions. *Trends Biochem. Sci.* **25**, 126-132.

Figure 67. Ball and stick representation of the generated conformation of the 1*H*-6-NI "prodrug" bound to the MAO-B active site. The residues forming the aromatic cage (Tyr398, Tyr435 and flavin) are shown in purple and the remaining key active site residues are shown in blue. The "prodrug" is shown in orange with rotatable bonds labeled in red. The sulfur atom of Cys172 is shown in green and the oxygen atom of Tyr188 is shown in green/blue.

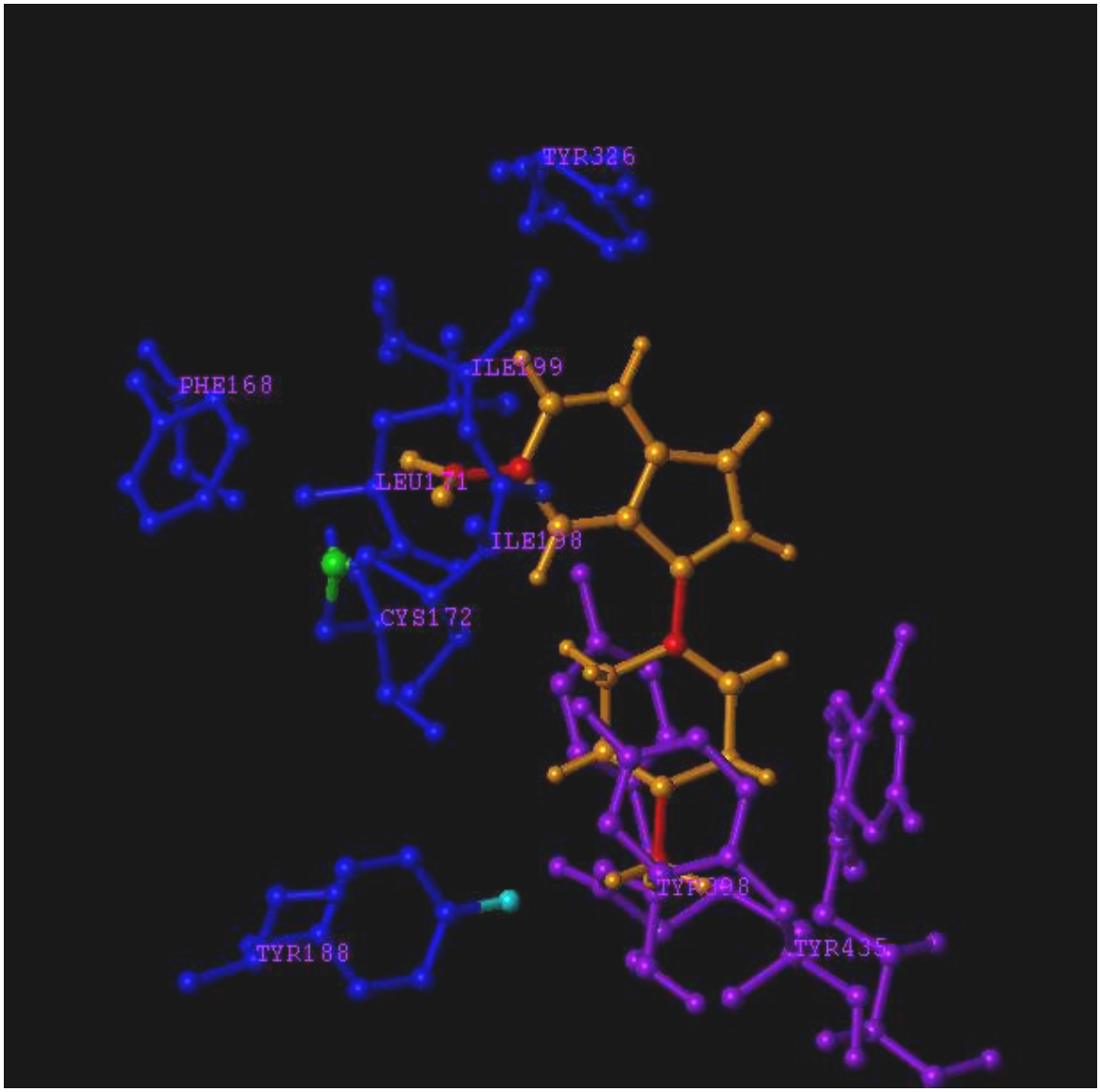

As shown in Figure 67, the tetrahydropyridinyl nitrogen of the 1*H*-6-NI "prodrug" is placed between two tyrosine residues (Tyr398 and Tyr435) which, together with flavin, constitute the aromatic cage proposed to be responsible for amine recognition. It is

possible that Tyr188 may be stabilizing this orientation further via hydrogen bonding. The nitro group is situated in the pocket formed by the residues Leu171, Ile198 and Ile199. The cysteine residue towards the lower end of the pocket, may be involved in hydrogen bonding interactions with the nitro group. The favorable "fit" of the 1*H*-6-NI "prodrug" is shown in Figure 68 as a space filling representation.

Figure 68. Space filling representation of the generated conformation of the 1*H*-6-NI "prodrug" bound to the MAO-B active site. The flavin is at the back, the Leu171, Ile198, Ile199 pocket is in the front. The residues forming the aromatic cage (Tyr398, Tyr435 and flavin) are shown in purple and the remaining key active site residues are shown in blue. The "prodrug" is shown in orange with rotatable bonds labeled in red.

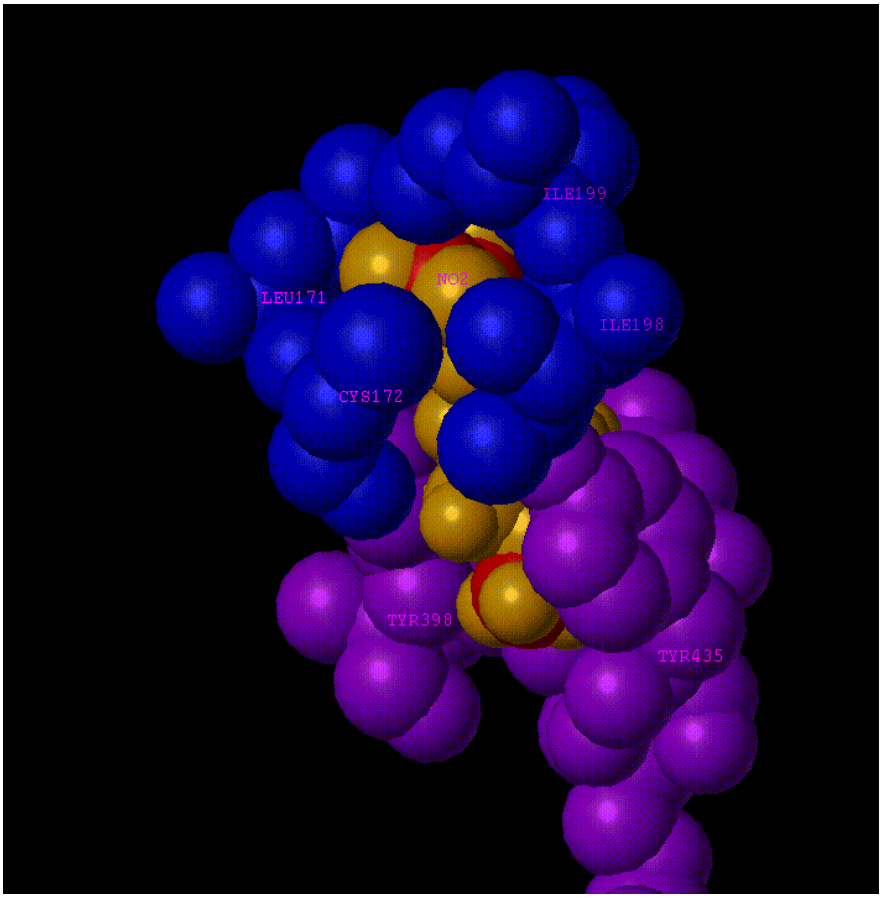

5.4.3. Docking of the 2*H*-7-NI "Prodrug"

Previously, the non-substrate properties of the 2*H*-7-NI "prodrug" **28** had been rationalized based on the length of the molecule along its main axis compared to the length of the active site model. Docking studies were carried out to explore further this proposal. A space filling representation of the generated binding conformation of **28** where the α-carbon is located close to N5 of flavin is shown in Figure 69. It is likely that the interaction of the phenyl ring of the indazolyl moiety with Tyr326 is contributing to the non-substrate properties of this compound since these two moieties occupy partially the same space in the generated model.

Figure 69. Space filling representation of the generated binding conformation of 2*H*-7-NI "prodrug" to MAO-B active site. The residues forming the aromatic cage (Tyr398, Tyr435 and flavin) are shown in purple. Tyr326, defining the length of the active site, is shown in blue. The "prodrug" is shown in orange with nitro group in green.

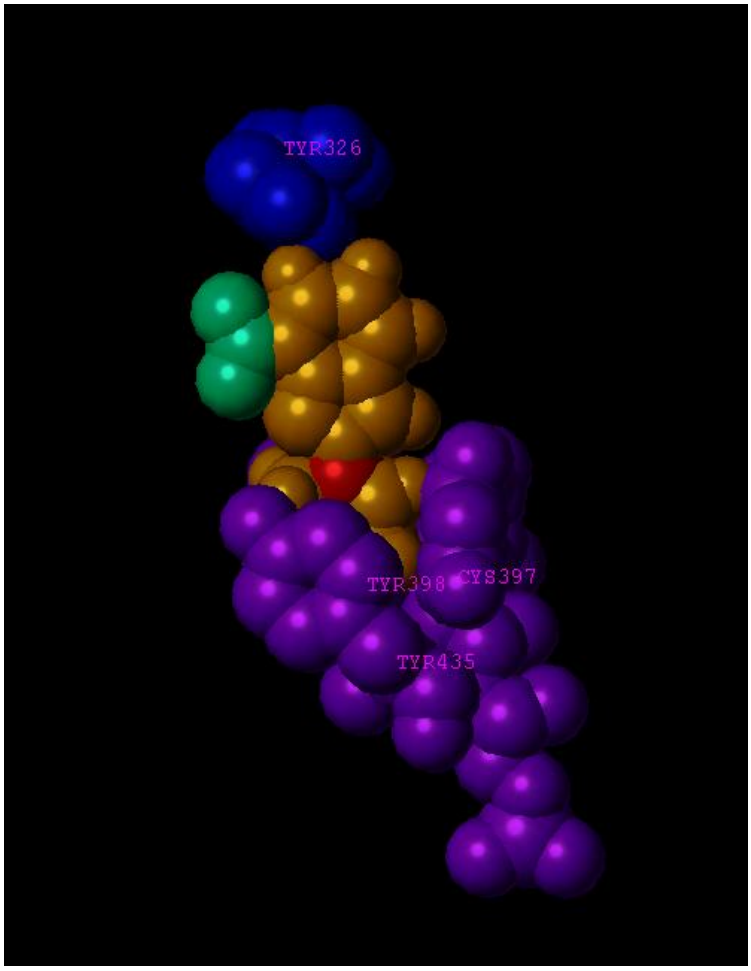

The binding conformation of 2*H*-7-NI "prodrug" **28** shown in Figure 69 was overlapped with the binding conformation of the 1*H*-6-NI "prodrug" **46** via alignment of the flavins (Fig. 70). The main difference between the orientation of the two "prodrugs" in the active site is the unfavored interaction of **28** with Tyr326 and the favored interaction of the nitro group of **46** with Cys172 located in the Leu171, Ile198, Ile199 pocket which is not present for the nitro group of **28**.

Figure 70. Comparison of the binding conformations of 28 and 46. The residues forming the aromatic cage (Tyr398, Tyr435 and flavin) are shown in purple. Tyr326 is shown in blue. "Prodrug" 28 is shown in orange and 46 in green with rotatable bonds labeled in red.

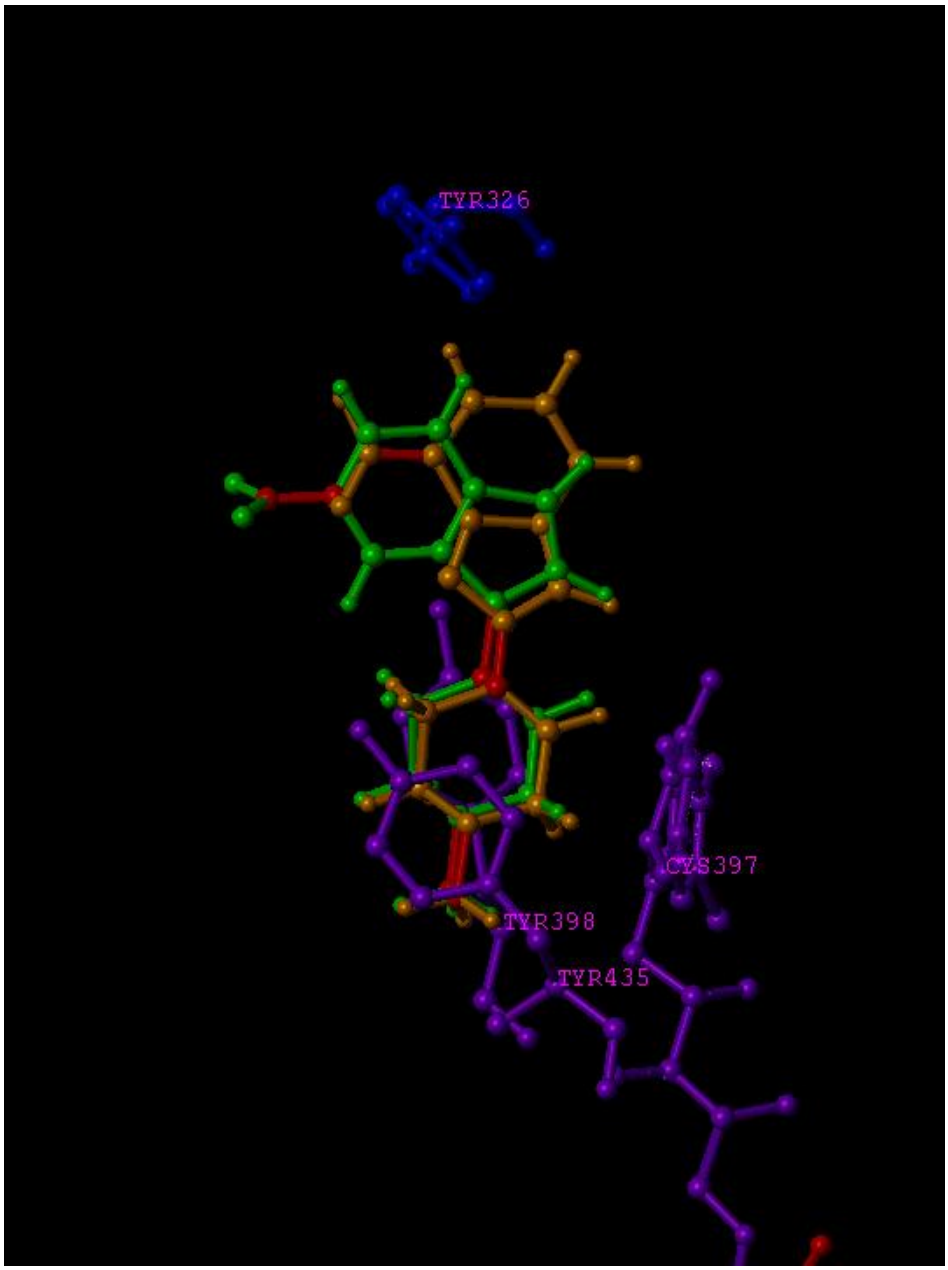

An alternative low energy binding conformation of **28** generated during the docking studies is shown in Figure 71. In this binding conformation, the indazole moiety is extended towards the entrance cavity. The α-carbon of the tetrahydropyridinyl moiety is oriented far from the N5 of flavin in agreement with the inhibitory properties of **28**.

Figure 71. Ball and stick representation of the generated alternative binding conformation of the 2*H*-7-NI "prodrug". The flavin is shown in purple. The three of the four active site residues separating the substrate cavity from the entrance cavity Leu171, Ile199, Tyr326 are shown in blue. "Prodrug" is shown in orange with rotatable bonds labeled in red.

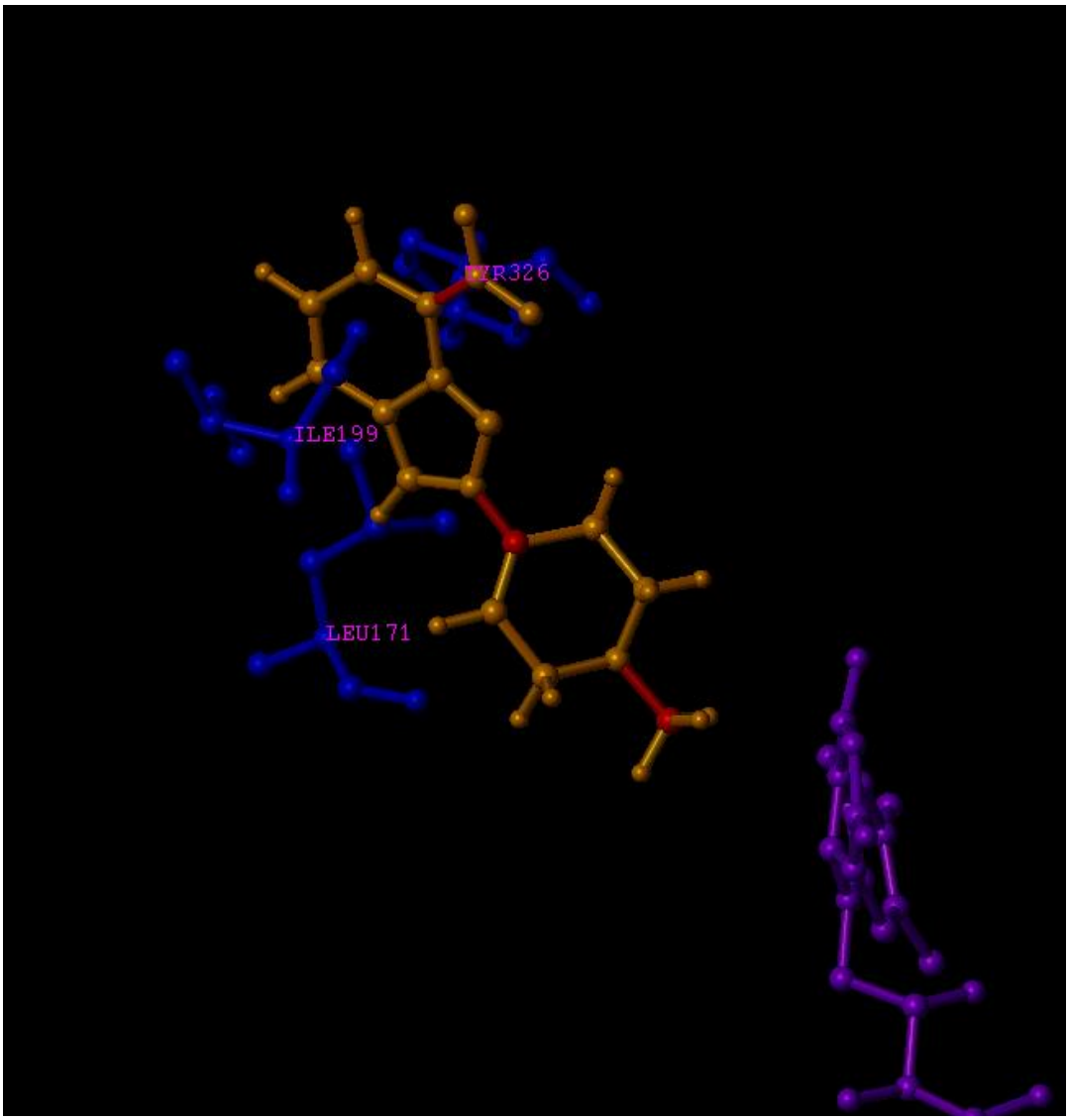

An example of an MAO-B inhibitor extending into the entrance cavity has been reported by Edmondson for *trans*-1,4-diphenyl-2-butene (**259**).[253] The x-ray crystal structure of MAO-B in complex with **259** shows that one of the phenyl groups occupies the entrance cavity and the second one occupies the substrate cavity (Fig. 72).

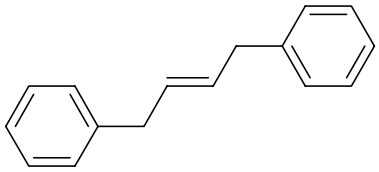

259

[253] Hubalek, F., Binda, C., Li, M., Mattevi, A., Edmondson, D.E. (2003) Polystyrene microbridges used in sitting-drop crystallization release 1,4-diphenyl-2-butene, a novel inhibitor of human MAO B. *Acta Crystallogr. D Biol. Crystallogr.* **59**, 1874-1876.

Figure 72. Ball and stick representation of the MAO-B active site in complex with inhibitor 259. The flavin is shown in purple. For clarity purposes only 4 of the residues lining the substrate cavity are shown and labeled in red. The residues separating the entrance cavity from the substrate cavity Phe168, Leu171, Ile199 and Tyr326 are shown in green. The residues lining the entrance cavity are shown in blue. Inhibitor 259 is shown in orange.

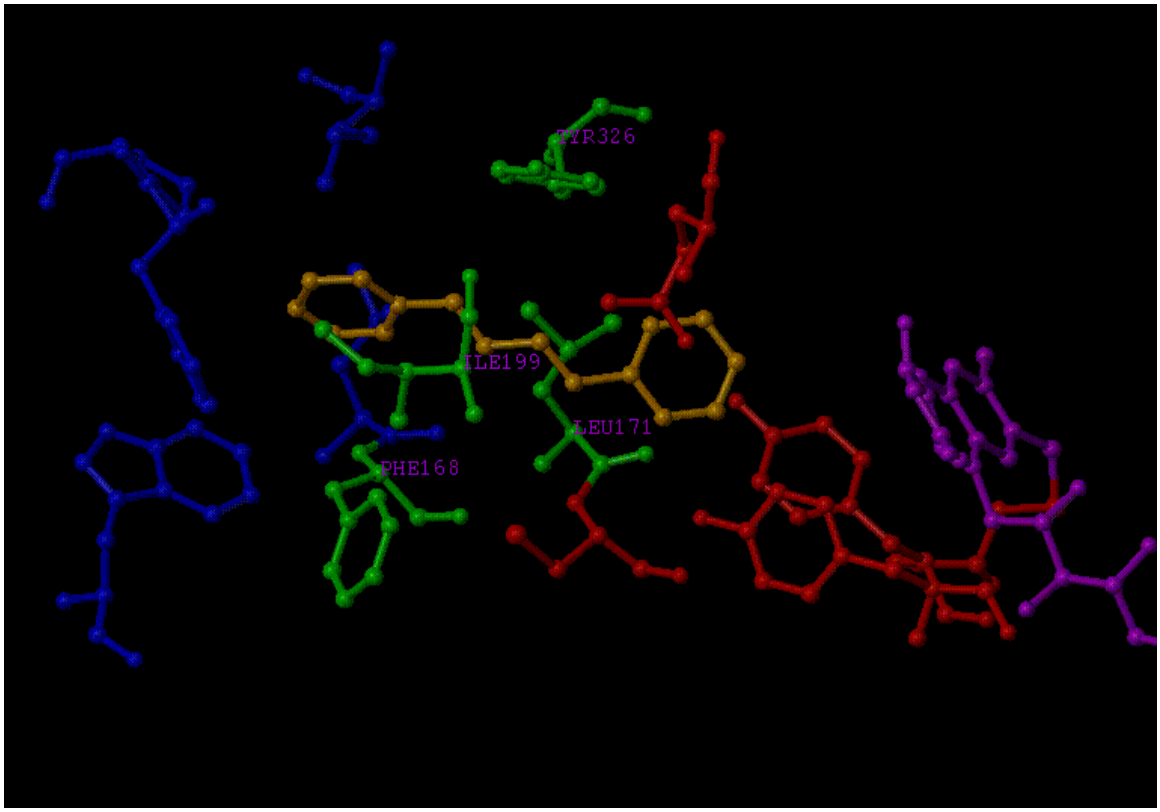

It is important to note that in the x-ray crystal structure of MAO-B in complex with **260**, the side chain of Ile199 rotates and "opens the gate" between the entrance cavity and the substrate cavity. In the case of MAO-B in complex with isatin "the gate is closed" (Fig. 70).[254]

[254] Binda, C., Hubalek, F., Li, M., Restelli, N., Edmondson, D.E., Mattevi, A. (2003) Insights into the mode of inhibition of human mitochondrial monoamine oxidase B from high-resolution crystal structures. *Proc. Natl. Acad. Sci.* **100**, 9750-9755.

Figure 73. Comparison of the orientation of the residues separating the substrate cavity from the entrance cavity (Phe168, Leu171, Ile199 and Tyr326) in the x-ray crystal structures of MAO-B in complex with *trans*-1,4-diphenyl-2-butene (259) and isatin (246). The flavin is depicted in purple. The residues separating the two cavities are shown in green for the x-ray crystal structure in complex with 259 and in red for the x-ray crystal structure with 246. Compound 259 is shown in orange and compound 246 is shown in blue.

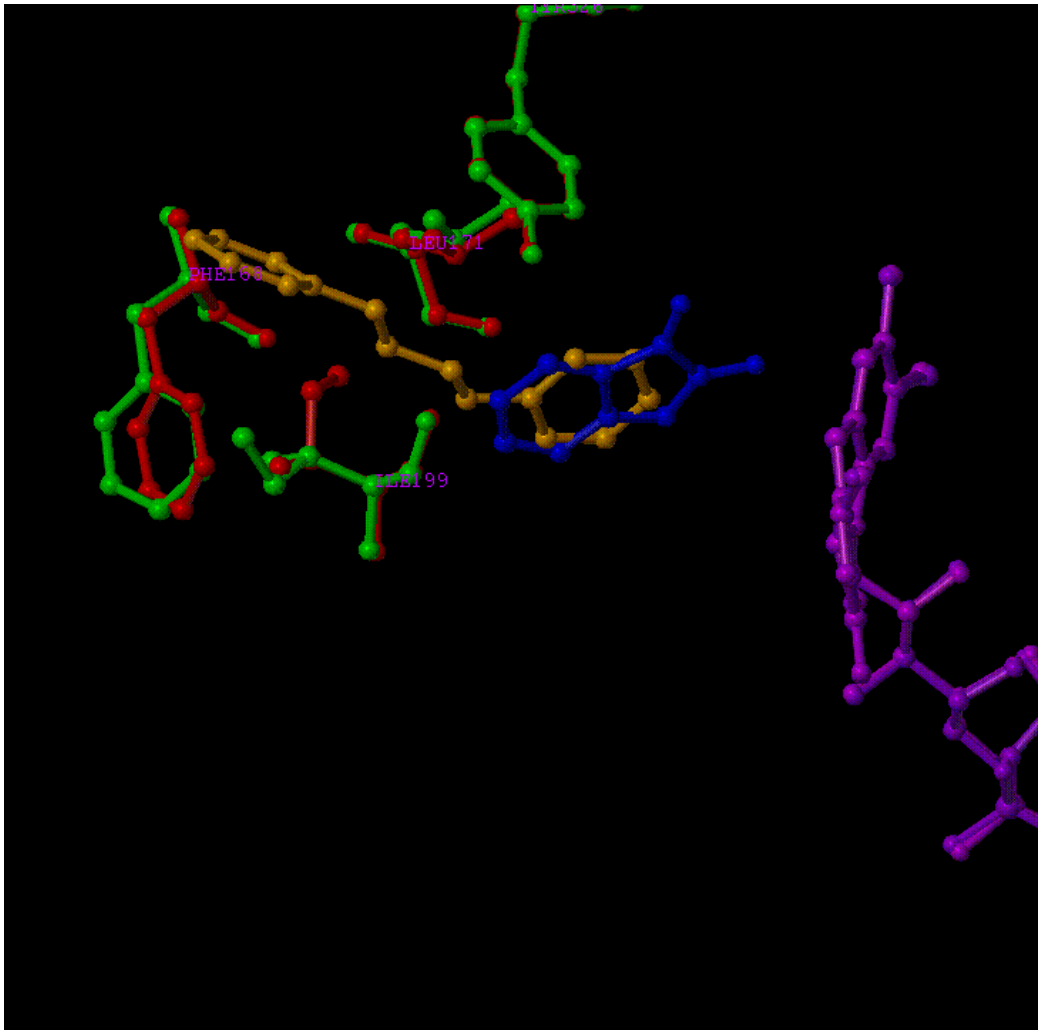

The literature evidence provides additional support for the possibility that the 2*H*-7-NI "prodrug" assumes an alternative binding conformation in the active site that extends into the entrance cavity. Indeed, overlap of the generated binding conformation for the 2*H*-7-NI "prodrug" with the x-ray crystal structure of MAO-B in complex with

259 is in agreement with this proposal (Fig. 74). However, it must be noted that the coordinates of the MAO-B crystal structure in complex with isatin was used for the docking studies where Ile199 gate "is closed". Therefore docking studies using the coordinates for the x-ray crystal structure of MAO-B in complex with **259** is expected to provide more accurate information regarding the inhibitor orientation of the 2*H*-7-NI "prodrug" as well as the orientation of other inhibitor molecules which may be extended into the entrance cavity.

Figure 74. Comparison of the generated binding conformation of 2*H*-7-NI "prodrug" with the x-ray crystal structure of MAO-B in complex with *trans*-1,4-diphenyl-2-butene (259). The flavin is depicted in purple. The residues separating the two cavities are shown in green for the x-ray crystal structure in complex with 259 and in blue for the generated binding conformation. The 2*H*-7-NI-prodrug is shown in orange and compound 259 is shown in red.